iJRASET
International Journal For Research in Applied Science and Engineering Technology

INTERNATIONAL JOURNAL FOR RESEARCH

IN APPLIED SCIENCE & ENGINEERING TECHNOLOGY

Volume: 10 **Issue:** III **Month of publication:** March 2022

DOI: https://doi.org/10.22214/ijraset.2022.41095

www.ijraset.com

Call: 08813907089 | E-mail ID: ijraset@gmail.com

International Journal for Research in Applied Science & Engineering Technology (IJRASET)
ISSN: 2321-9653; IC Value: 45.98; SJ Impact Factor: 7.538
Volume 10 Issue III Mar 2022- Available at www.ijraset.com

Analytical and Numerical Correlation of Hertz Contact under Elastic and Plastic Regime

Puneeth M L[1], Dr. G. Mallesh[2]
[1]*Research Scholar, JSS Science and Technology University, Mysuru*
[2]*Professor, JSS Science and Technology University, Mysuru*

Abstract: ***The contact of two bodies is found in many engineering applications. Some of the best examples are Hardness Testing, contact between ball bearings in races, Head –Disk interaction in storage devices, Impact of dust and other particles on Fan blades in a gas turbine and in Sports, especially where ball contact is dominant (like Golf, Hockey, Snooker etc.). The major characteristics of the problem are the localized deformation and the variation in the contact area with the contact force. The contact force–displacement relationship is nonlinear and high stresses are often generated. Therefore, plastic deformation is likely to occur for most engineering contact problems. This paper tries to simplify and concise the hertz contact behaviour under both Elastic and Plastic regime, which helps for better understanding in designing various contact parts.***
Keywords: Abaqus, Axi-symmetric, Hertz Contact, Implicit solver, Matlab.

I. INTRODUCTION

The Hertzian contact solution is a fundamental component of elastic contact mechanics, with applications ranging from geotechnical applications such as determining the load bearing capacity of soil to determining the fatigue life of bearings, gears, and other structures having two surfaces in contact. These contact domains at any system's interface are critical because they facilitate load transfer from one component to another. To improve the design of components in such locations, knowledge of the contact characteristics between the interfaces is essential. Spherical components in contact are a variant of the Hertz contact, which occurs when two spheres or a sphere and the surface of a half space comes in contact. Because the contact area is theoretically a "point" preceding load application, this sort of contact is also known as a point contact. When the bodies deform under load, the contact area becomes a "circular area," getting this the term "circular contact." If the components in contact have three-dimensional geometries, such as balls in a rolling-element bearing, and this contact could be reduced into an interaction that can occur between two ellipsoidal bodies that would be determined by the orthogonal principal radii of curvature which is also highlighted in Fig. 1.

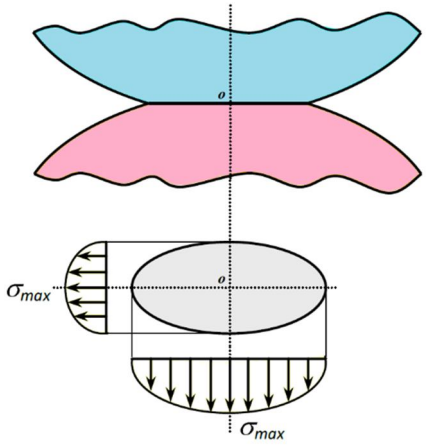

Fig. 1 Two bodies in contact with Elliptical Stress distribution

The contact problem's main characteristics are localized deformation and contact area variations that is proportional to contact force. Also, the relationship between force and displacement is highly non-linear due to onset and progression of plastic deformation. Significant amount of work has been carried out by many researchers on elastic-plastic deformation of two bodies in contact and their effect on strength and performance on the life of component. The analysis of stress distribution and residual stresses are important for better understanding of the behaviour and optimization of design.

The first extensive work on contact was carried out in the year 1882 by Hertz [1], while studying on Newton's optical interference fringes arising from gap between two glass lenses in contact. The work satisfactory analysed the stresses arising due to the contact of two elastic solids. This hypothesis showed that the contact pressure across the contact area is generally elliptically. Hertz's theory provides a good approximation of contact of hard bodies where contact region remains small when compared with the size of the bodies. Also, the solution is not restricted to a specific material or geometry.

Johnson, K.L., [2] proposed a model for the contact of a rigid sphere and an elastic–perfectly plastic half-space, assuming fully developed plastic flow from which the contact force–displacement relationship for static contact and the coefficient of restitution for impact can be calculated. Experiment work was also conducted on contact of spheres on a rigid flat plate and this showed that there was permanent deformation on both spheres and flat surfaces. An alternative model was suggested by Thronton [3] which described the contact pressure distribution as approximated by an ''elastic" phase during which the pressure distribution was Hertzian, followed by a ''plastic" phase during which the pressure distribution was described by a truncated Hertzian pressure distribution by defining a ''limiting contact pressure". An Elasto-plastic normal force–displacement (NFD) model was developed by Vu-Quoc et al., [4] in which the contact radius was decomposed into an elastic part and a plastic part. The contact curvature was corrected by using an adjustable coefficient to account for the effect of plastic deformation. Proposed NFD model led to more accurate coefficient of restitution, which was a function of velocity of two bodies in collision. The process of loading and unloading of two dissimilar elastic-plastic spheres and with rigid spheres for very large indentation was carried out by Mesarovic [5]. They assumed that during unloading process the deformation is mainly elastic whilst neglecting the friction. The effect of yield strain and the size of the spheres were also analysed. Strain hardening effect was also considered in their analysis. A series of numerical analysis was conducted Quicksall et al.,[6] for various mechanical properties of the contact model. Young's modulus and Poisson ratio were varied keeping the yield strength as constant. FEM results also showed the material dependence on contact area. Analysis showed that non-dimensional contact area increases with increase in Poisson's ratio and with increase in Modulus of elasticity, the value of load increases in plastic range. Jackson & Green [7] developed their own models for hemispherical contact with a rigid flat. They showed that their results for interference, contact area and contact force, so that these non-dimensional values equal unity at the onset of yielding. Suitable expression to relate the dimensionless mean contact pressure, dimensionless contact load and the dimensionless contact area with the dimensionless interference ratio were studied. A brief study on the residual stresses and strains obtained after an elastic-plastic deformation was done by Jackson et al., [8]. They showed that the maximum residual stress transitioned from an area below the contact region along the axis of symmetry. The results highlighted that the fully plastic contact pressure is approximated as a constant factor which was about the three times the yield strength which varied with deformation, which in turn depends on material property. A brief study on the elastic-plastic transition behaviour was conducted by Shankar et al., [9] accounting for the effect of realistic material behaviour in terms of the varying yield strengths and the isotropic strain hardening behaviour. They showed that yield strength and tangent modulus has influence on transition from elastic to plastic deformation. The strain hardening effect for elastic-plastic loading and un-loading was analysed by Sahoo & Chatterjee [10] and it was observed that with the increase in strain hardening, the resistance to deformation of a material is increased and the material becomes capable of carrying higher amount of load in a smaller contact area. They also showed that contact force and area depend on modulus of elasticity.

While the above authors and their work provided the fundamentals basics for tackling the hertz problem with different contact model for analyzing, other few authors mentioned below highlighted the different applications of Hertz contact, which is described in brief. Ligia Cristina [11] analysed the contact stresses arised due to two cylindrical bodies with parallel axes, which outlined that the contact surface was an ellipse, and would gradually transforms into a circular surface in extreme loading conditions. The material in the proximity of the contact ellipse is compressed relatively uniformly in all directions and can withstand high loads without deformations. Hariprasad et al., [12] Evaluated the Hertzian contact parameters through displacement field in the vicinity of the contact zones which was based on complex potential approach. Experiments were conducted to evaluate the contact zone using the whole field displacement parameters. Gourgiotis et al., [13] revisited the Hertz contact problem based on the couple-stress elasticity. The aim is to see how well this gradient theory describes the indentation response and related size effects in microstructure materials such as bone tissues, cellular polymers, ceramics, composites, foams, masonry. Sirata et al., [14] studied on the rail-wheel contact under Tangential & normal loading by utilizing the Hertz formulation. To simulate the material's behaviour under the applied load, separate elastic and elastoplastic material models were utilized. Handbook of Contact Mechanics by Popov et al., [15] is recommended for further reading and through understanding of the concept. this is a comprehensive open access reference book which deals with axially symmetrical contact issues and Exact solutions for industrial and research applications.

ISSN: 2321-9653; IC Value: 45.98; SJ Impact Factor: 7.538
Volume 10 Issue III Mar 2022- Available at www.ijraset.com

II. MATHEMATICAL MODEL OF HERTZ CONTACT

The Hertz contact solution has been extensively applied as the foundation for the spherical indentation testing technique, which is widely used for material property assessment and characterization of deformation behaviour. In the perspective of a generalised continuum theory, the current research expands the traditional Hertz contact solution.

A. Elastic Compression Phase

Consider the normal contact between the two spheres as shown in Fig. 2. Here, the solid and dashed line shows the bodies before and after loading.

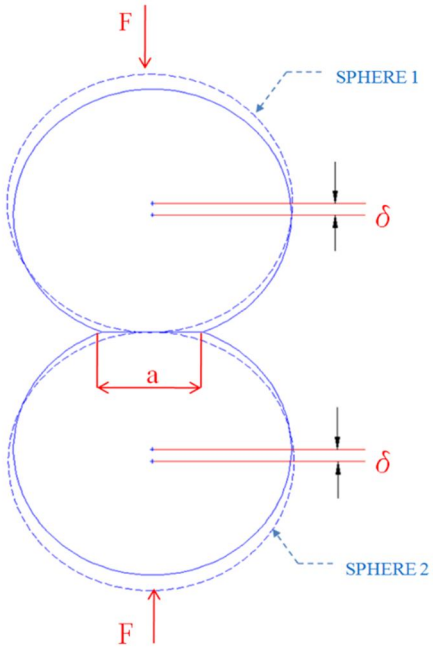

Fig. 2 Two spheres in contact, subjected to normal Force F

The contact force and contact radius can be expressed as follow:

$$a = \left(\frac{3FR}{4E}\right)^{1/3} \qquad \text{.....1}$$

$$\delta = \left(\frac{3F}{4aE}\right) \qquad \text{.....2}$$

where, δ is the deformation, R is the effective radius and E is the Hertz elastic modulus and is given by $R^{-1} = R_1^{-1} + R_2^{-1}$ and $E = [(1-\vartheta_1^2)/E_1 + (1-\vartheta_2^2)/E_2]^{-1}$ respectively, F and a are the contact force and contact radius respectively. This can be further classified based on the dimension as given below:

Case-1 for $0 < R_2 < \infty$ the effective radius $R^{-1} = R_1^{-1} + R_2^{-1}$

Case-2 for $R_2 = \infty$ and $E_2 = \infty$ which is a typical rigid flat body.

The effective radius and Hertz elastic modulus is given by $R = R_1$ and $E = E1/(1-\vartheta^2)$. For both cases analytical solution is taken from equation 1 and 2 , Contact force and Contact area can be simplified as :

$$a = \sqrt{\delta R} \qquad \text{.....3}$$

$$F = \frac{4}{3} E\sqrt{R}\delta^{3/2} \qquad \text{.....4}$$

ISSN: 2321-9653; IC Value: 45.98; SJ Impact Factor: 7.538
Volume 10 Issue III Mar 2022- Available at www.ijraset.com

B. Elliptical distribution of Hertz contact pressure

According to Hertz law, the pressure distribution over the contact surface is elliptical and is expressed as follows,

$$p(r) = p(0)(a^2 - r^2)^{1/2} \quad \text{.....5}$$

where r is a radial coordinate, When $r = 0$ i.e. at the contact centre maximum pressure in terms of contact force and contact radius is given by

$$p(0) = {}^{3F}/_{2\pi a} \quad \text{.....6}$$

Equation 6 shows that maximum pressure at the centre is 1.5 times the average pressure due to contact force. Eliminating δ from equation 3 and 4 contact force in terms of contact radius is written as

$$F = {}^{4Ea}/_{3R} \quad \text{.....7}$$

Using equation 5 and 7 the distribution of pressure along contact radius is given by

$$p(r) = \frac{2E}{\pi R}(a^2 - r^2)^{1/2} \quad \text{.....8}$$

Thus contact radius in relation with maximum contact pressure at the centre is $\pi Rp(0)/2E$ and at the onset yielding contact radius, force and deformation can be written as

$$a_y = \frac{\pi R p_y}{2E} \quad \text{.....9}$$

$$F_y = \frac{4ER^2}{3}\left(\frac{\pi p_y}{2E}\right)^3 \quad \text{.....10}$$

$$\delta_y = R\left(\frac{\pi p_y}{2E}\right)^2 \quad \text{.....11}$$

Where p_y, a_y and δ_y are pressure, contact radius, and deformation at the onset of yielding respectively. When contact pressure force exceeds the maximum elastic contact force material yields and plastic deformation develops. The maximum pressure is given by $p_o = c\sigma_y$, where c is the yield strength constant and follows an elliptical path.

C. Elastic Perfectly Plastic Compression Phase

Contact force during elastic perfectly plastic compression assumes constant pressure up to contact radius a_y and there after pressure distribution depends on Hertz contact pressure as shown in Fig. 3, mathematically it can be expressed as

$$p(r) = \begin{cases} p_0 & 0 \le r \le a_p \\ \frac{2E}{\pi R}(1 - ({}^{r}/_{a})^2)^{1/2} & a_p \le r \le a \end{cases} \quad \text{.....12}$$

Where a_p is the radius of contact over which a uniform pressure is assumed and is defined as

$$a_p = a\left[1 - \left(\frac{\pi p_o R}{2Ea}\right)^2\right]^{1/2} \quad \text{.....13}$$

The contact force at the Elastic-Plastic regime is expressed as

$$F = \pi R p_o \delta - \frac{\pi^3 {p_o}^3 R^2}{12E^2} \quad \text{.....14}$$

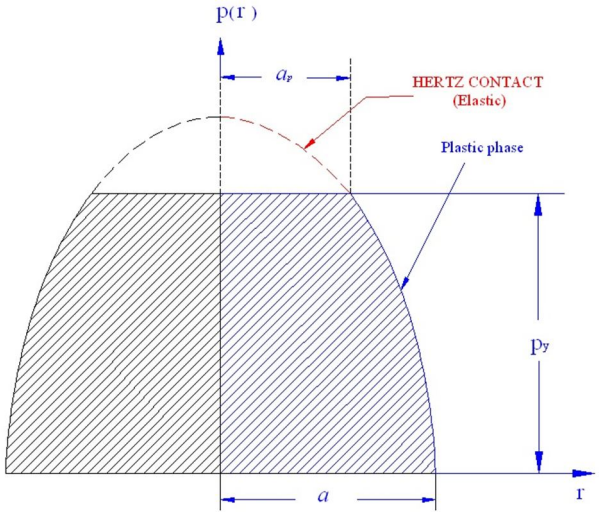

Fig. 3 Pressure distribution curve, Elliptical in Nature

D. Unloading of Spherical Contact after Elastoplastic Deformation

Unloading of loaded specimen is an important problem, because of restitution it gives a different relation between contact force and displacement the unloading and subsequent reloading are perfectly elastic and for the same contact force the unloading and the following reloading will produce identical pressure distribution, contact radii and displacement. The contact force in elastic recovery phase is given as

$$F = \frac{4}{3}E\sqrt{R_{res}}(\delta - \delta_{res})^{3/2} \qquad \text{.....15}$$

Where δ_{res} is the residual deformation and R_{res} is the effective radius after the elastic phase and is given as

$$R_{res} = \frac{4E(\delta_{max}R)^{3/2}}{3F} \qquad \text{.....16}$$

Since, contact force at end of the elastic perfectly plastic compression phase and in the beginning of the elastic recovery phase is equal, therefore

$$\frac{4}{3}E\sqrt{R_{res}}(\delta_{max} - \delta_{res})^{3/2} = \pi R p_o \delta_{max} - \frac{\pi^3 {p_o}^3 R^2}{12E^2} \qquad \text{.....17}$$

Solving the equation 17 residual deformation is given as

$$\delta_{res} = \delta_{max} - \left[\frac{3}{4E\sqrt{R_{res}}}\left[\pi R p_o \delta_{max} - \frac{\pi^3 {p_o}^3 R^2}{12E^2}\right]\right]^{2/3} \qquad \text{.....18}$$

E. Radial and Axial Stresses at Contact Surface

Stresses are also compared in this phase. According to basic theory $\sigma_r = \sigma_\theta$ and σ_z is compared with analytical the following graphs shows comparison between analytical stresses and FEM results. The following analytical equations were used for stress comparison.

$$\frac{\sigma_r}{p_o} = \frac{\sigma_\theta}{p_o} = -(1-\vartheta)\{1 - (z/a)\tan^{-1}(a/z)\} + \frac{1}{2}(1 + (z/a)^2)^{-1} \qquad \text{.....19}$$

$$\frac{\sigma_z}{p_o} = -(1 + (z/a)^2)^{-1} \qquad \text{.....20}$$

ISSN: 2321-9653; IC Value: 45.98; SJ Impact Factor: 7.538
Volume 10 Issue III Mar 2022- Available at www.ijraset.com

III.FINITE ELEMENT ANALYSIS

A. Geometrical Model & Material Details

Two spheres of radius R= 0.1 m with contact surface defined to each of the sphere is considered. The material of both spheres is considered to be steel, and the material details are highlighted in the below table:

TABLE I
MATERIAL PROPERTY OF CONTACT BODIES

Material	Density (Ton/mm3)	Young's modulus (MPa)	Poisson's ratio	Yield stress (MPa)
Structural Steel	7.850e-09	200000	0.32	210

B. Boundary Conditions

Displacement of 4mm is applied to the sphere with a constant rate and then removed. To simulate the contact behaviour between the two spheres, a contact pair interface is created, in which friction is negligible. The loading and un-loading is performed by using a time-controlled displacement increment method. ABAQUS-6.14 [15] is used as a solver and meshing is done by commercial package HYPERMESH. Implicit solver based on static approach is utilized. Since the model can be considered as axisymmetric, Abaqus element formulation *CAX4R* was utilized (Continuum axisymmetric 4 node reduced integral element type) which also helps to improve the efficiency of computation. Due to localized stresses and deformation during the contact phenomenon, a very fine mesh is used around the contact centre and coarse mesh away from the centre as highlighted in Fig. 4. Rotating quad elements were used to achieve the transition between coarse mesh to fine mesh. Five layered mesh transition approach was utilized to achieve finer mesh at the region of the contact. This helps to avoid numerical error caused by sudden change in mesh size and there is a gradual increase in element size in between these two regions This was achieved based on mesh convergence study conducted to get better results that would tend to correlate closely with analytical results. The convergence study has been carried out by using various mesh density and mesh is chosen in such a way that the computational cost and time will be as low as possible and also would give accurate numerical results. Using Symmetric Contact Pairs and refined mesh on both interfaces, penetration between the Master and Slave surfaces was reduced to a minimum.

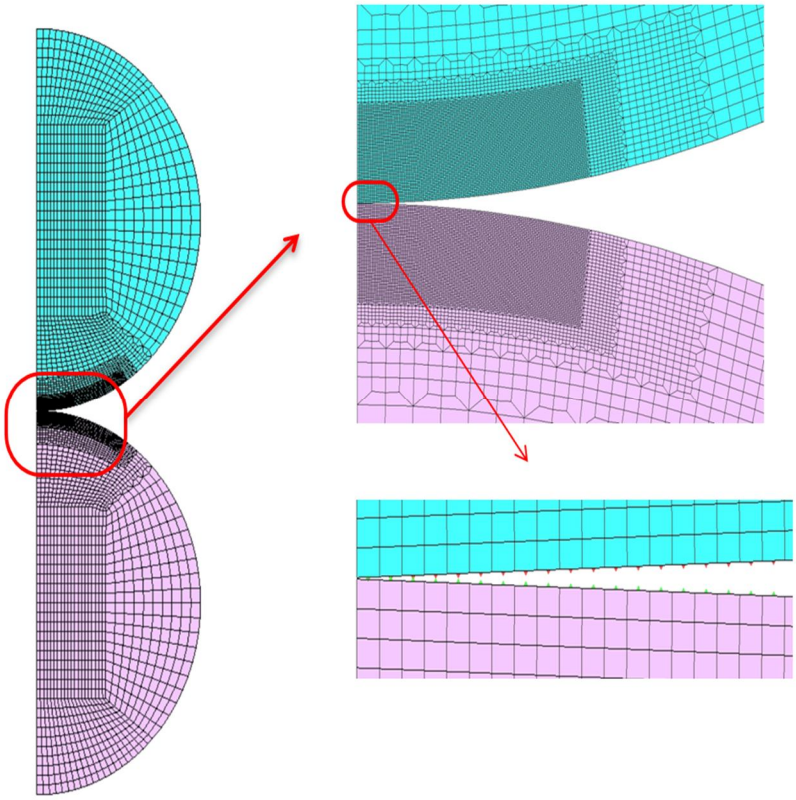

Fig. 4: Axi-Symmetric Meshed model of two spheres (Fine mesh at contact region)

ISSN: 2321-9653; IC Value: 45.98; SJ Impact Factor: 7.538
Volume 10 Issue III Mar 2022- Available at www.ijraset.com

IV. RESULTS AND DISCUSSION

To demonstrate the results pertaining to elastic contact pressure distribution, the relationships between pressure on the contact surface, contact radius and Displacement are examined prior to the yield. After yielding, plastic deformation occurs. After the force exceeds elastic limit, the contact can be divided into two stages. One is called the Elasto-plastic contact in which the maximum pressure at the contact center increases gradually from $1.6\,\sigma_y$ to about $3\,\sigma_y$. Other is called fully plastic contact in which the pressure does not appear to increase further, but they will be enlargement of contact area.

The results obtained from the finite element analysis are compared analytically by using MATLAB software. Results and correlations of contact pressure distribution, relationship between contact force, displacement and contact radius during elastic-plastic loading and unloading is as shown in the result sections. The results show that the deformation during unloading from a contact beyond the Elastic limit is perfectly plastic. However, the pressure distribution returns to the Hertzian elliptical distribution only when the maximum pressure at the contact center is below $1.6\,\sigma_y$. The agreement between finite element and analytical results are closer.

A. Elastic Loading

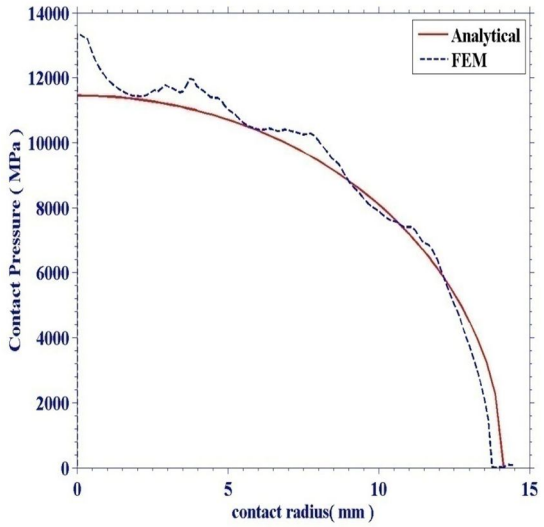

Fig. 5 Pressure distribution on the contact surface

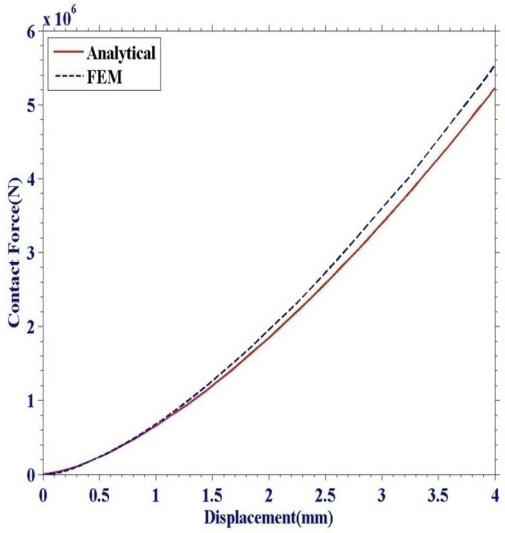

Fig. 6 Elastic regime contact behaviour

The pressure distribution on the contact surface is highlighted in Fig.5. The variation in the FEM result at the initial contact time-step is attributed to the finer element at the contact zone that have been experiencing concentrated pressure. This eases out when the contact area increases gradually and has a good correlation with the analytical result. Fig. 6 shows a good agreement between Normal Force F versus Displacement δ within the elastic limit of the material. In purely elastic compression, the material behaves on same line of the elastic path of stress-strain curve with no yielding and no plastic deformation. Loading and unloading follow same path hence there is no energy loss.

B. Plastic Loading

As the load increases beyond the elastic limit, material starts to yields and by assuming the phenomenon to be elastic-perfectly plastic, force and displacement is calculated which is highlighted in Fig. 7. Since the plastic deformation inclines to flatten out the surface which produces a larger contact area. It was observed that high residual stress presides near to the material pile up formed during plastic deformation. Hertz calculations suggest a nonlinear pressure-over-closure relationship between two contacting solids in principle. In particular, when the distance between the two surfaces is closed, the contact stiffness decreases with pile up of residual stresses and deformation.

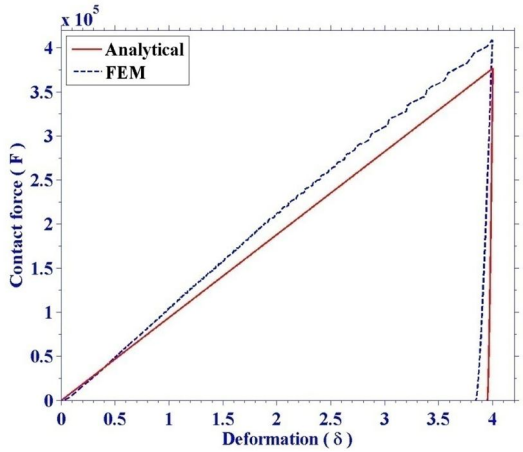

Fig. 7 Plastic regime contact behaviour

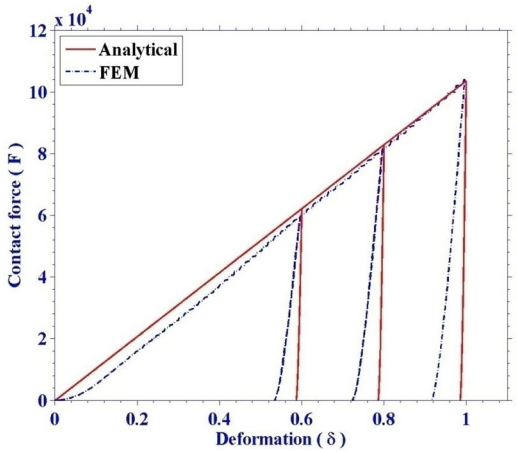

Fig. 8 Repeated loading and unloading

The above Fig. 8 highlights the graph of force-displacement. It can be clearly observed that unloading curve which follows the different path and gives the residual stress deformation with accumulated deformation. Both FEM and analytical results are in close agreement. In unloading case after certain cycles, the curve follows different path due to strain hardening relaxation, which leads to no change in the load carrying capacity in spite of plastically deformed.

C. Comparison of Radial and Axial Stress

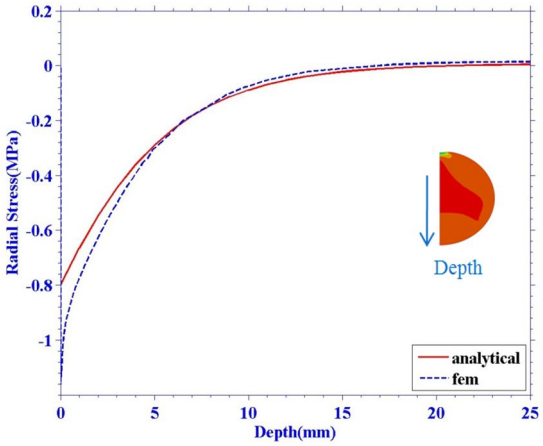

Fig. 7 Radial Stress along depth

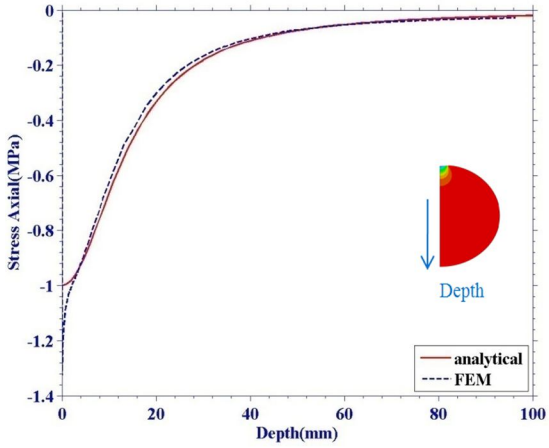

Fig. 8 Axial stress along depth

The Fig. 9 shows the variation of radial stresses along the z-direction for various loading conditions. It's clearly observed that, as the distance along z-direction the stresses gradually come to mean position i.e. zero value. Fig. 10 shows the variation of Axial stresses along z-direction here one can clearly observe that there is a close encounter between analytical and FEM results. Just below the contact surface, high stress region starts to form. When the material yields eventually, it starts flowing plastically, since it cannot resist deformation.

V. CONCLUSIONS

Simplified analytical model for the calculation of Hertz contact was presented with both analytical and numerical correlation. The solution involves relationship between displacements, consecutive force arised and the Maximum pressure due to contact between the two bodies. Good correlation was achieved between the analytical model and with FEM analysis. The effect of strain hardening for elastic-plastic contact was also observed and was inferred that with the increase in strain hardening the resistance to deformation of a material is increased and the material becomes capable of carrying higher amount of load in a smaller contact area. It was also observed that for same contact area, the load carrying capacity increased with the increase in strain hardening during loading-unloading phenomenon.

Surface and subsurface stress fields for the interaction between two highly conforming Axi-symmetric materials were properly computed using FEM. This complex contact mechanics problem was solved using Abaqus software. Using enhanced contact controls, this was effectively modelled in Abaqus. An error of less than 5 % was observed between the theoretical and Finite element results. This successfully shows that Abaqus implicit solver is capable of solving axisymmetric and non-linear contact problem

REFERENCES

[1] H. Hertz, On the Contact of Elastic Bodies, J Pure Appl. Math. i 146–162,1896.
[2] K.L Johnson, Contact Mechanics. Cambridge University Press, 1985.
[3] Thornton, C, Coefficient of restitution for collinear collisions of elastic-perfectly plastic sphere, p. 383-386, 1997.
[4] Vu-Quoc, L., X. Zhang, and L. Lesburg. , A normal force-displacement model for contacting spheres accounting for plastic deformation: force-driven formulation. J. Appl. Mech. 67, no. 2, p. 363-371 ,2000.
[5] Mesarovic, Sinisa, and Norman A. Fleck, Frictionless indentation of dissimilar elastic–plastic spheres, International Journal of Solids and Structures 37, no. 46-47, p. 7071-7091, 2000.
[6] Quicksall, J. J., Jackson, R. L., & Green, I. Elasto-Plastic hemispherical contact models for various Mechanical properties, Journal of Engineering Tribology, 218, p. 313-322. 2004.
[7] Jackson, R. L., & Green, I. (2005). A Finite element study of Elasto-Plastic Hemispherical Contact against a Rigid Flat. Journal of Tribology, 127, 343-354.
[8] Jackson, R., Chusoipin, I., & Green, I, A finite Element study of the Residual Stress and Deformation in Hemispherical Contacts, Transaction of the ASME, 127, 484-493, 2005.
[9] Shankar, S., Mayuram,M.M., Effect of strain hardening in Elastic-Plastic transition behavior in a hemisphere in contact with a rigid flat, International Journal of Solids and Structures, 45, 3009-3020, 2008.
[10] Sahoo, P., & Chatterjee, B., Effect of strain Hardening on Unloading of a Deformable Sphere Loaded against a Rigid Flat. International journal of Engineering, 2(4), 225-233, 2010.
[11] Brezeanu, Ligia Cristina, Contact stresses between two cylindrical bodies with parallel axes: analysis by FEM, Acta Marisiensis. Seria Technologica 10, no. 2, 2013.
[12] Hariprasad, M. P., and K. Ramesh, Evaluation of Hertzian contact parameters from whole field displacement data, The Journal of Strain Analysis for Engineering Design 52, no. 7, p. 403-409, 2017.
[13] 13. Gourgiotis, P. A., Th Zisis, A. E. Giannakopoulos, and H. G. Georgiadis, The Hertz contact problem in couple-stress elasticity, International Journal of Solids and Structures 168 228-237, 2019.
[14] Sirata, G. G., Hirpa G. Lemu, Krzysztof Waclawiak, and Yohanis D. Jelila, Study of rail-wheel contact problem by analytical and numerical approaches, In IOP Conference Series: Materials Science and Engineering, vol. 1201, no. 1, p. 012035. , 2021.
[15] Popov, Valentin L., Markus Heß, and Emanuel Willert, Handbook of contact mechanics: exact solutions of axisymmetric contact problems, Springer Nature, 2019.
[16] Dassault Systèmes Simulia, Abaqus Analysis User's Manual, Version 6.14.

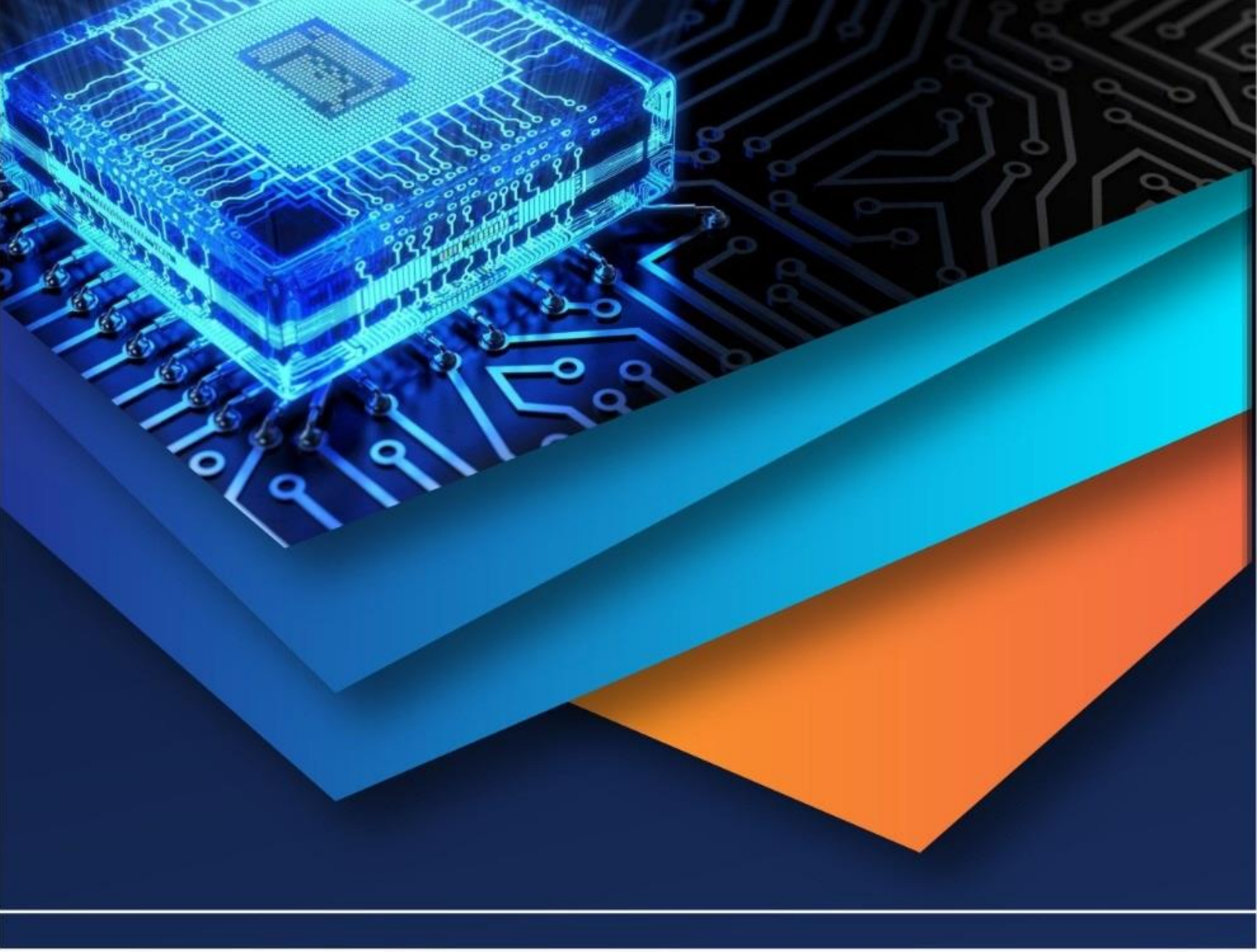

10.22214/IJRASET

45.98

IMPACT FACTOR: 7.129

IMPACT FACTOR: 7.429

INTERNATIONAL JOURNAL FOR RESEARCH

IN APPLIED SCIENCE & ENGINEERING TECHNOLOGY